BRAIN INJURY FROM THE MACRO TO THE MICRO LEVEL AND BACK AGAIN: WHAT HAVE WE LEARNED TO DATE?

Lawrence E. Thibault
Professor and Chairman
Department of Bioengineering
University of Pennsylvania

Introduction

This presentation is intended to relate the macroscopic with the more microscopic aspects of the biomechanics of central nervous system injury. A natural evolution in the field of injury biomechanics has taken place in recent years. Investigators have moved from the study of the macro to the micro world of biomechanics in order to obtain answers to the current questions of cellular and tissue failure criteria, as these relate to the macro issues of human injury tolerance criteria. A brief discussion of this topic is the purpose of this report. Elements of this presentation are found elsewhere in the literature.

The majority of our current concepts relating to the biomechanical aspects of human injury have come from research that may be described as macroscopic in nature. To this end human cadaver specimens, various animal models, anthropomorphic test devices, and both analytical and numerical simulations have served as the primary tools of investigation in our field to date. Collectively, the research findings from this endeavor have been responsible for the contemporary views of human injury tolerance criteria and they have led to numerous standards and regulations, and to the design of a safer mechanical environment.

The contributions of the biomechanics community in this regard have been enormous in the context of the overall national effort in injury control and prevention This should provide the reader with a sense of this achievement and an idea of how the macroscopic world of biomechanics has been the logical first step in estimating the effects of mechanical forces on the process of injury production and its sequelae.

This discussion is intended to focus upon an adjunct approach in the study of the biological effects of mechanical forces that are applied to living structures.

The approach utilizes isolated tissue and cell culture models and, therefore, may be considered more microscopic in contrast with the previously described research. It is simply another tool that the biomechanics community may employ to study this complex problem.

Investigations at the cellular and subcellular level have been prompted by the following:

A. to understand the relationship between the macroscopic descriptors of the applied loads (contact force, impact velocity, and acceleration) and the associated deformation of the tissue;

B. to relate the tissue deformation to the field variables such as strain in order to describe the dynamic mechanical environment of the cell;

C. to study the physiological or pathophysiological response of the cell to mechanical stimuli.

With the technology available today it is possible to measure the macroscopic loads that result from accident simulation with good precision. Further, using physical and mathematical models one can then estimate the deformations that occur at the organ or tissue level when an organism is subjected to these loads. It remains to develop the failure

criteria for the elements that consitute the living structures. With the experimental methodologies available in recent years it is now possible to subject isolated tissue and cell cultures to controlled mechanical stimulation and to measure the physiological and biochemical events that are elicited by the stimuli and may relate to the functional or structural failure of these components.

In this regard one may think of mechanical stimulation as another physical factor along with the chemical, electrical, and thermal conditions which in concert constitute the environment of the cell. As in these other cases it is reasonable to assume that mechanical stimulation when "excessive" (operating out of the physiological range) will lead to injury or possibly cell death.

This discussion is not intended as an exhaustive review of the research associated with the biomechanics of injury at the tissue or cellular level since much of this work is relatively new and is not readily available in the literature as of this time. Rather, this report is intended to serve as a description of a process whereby one can move from the macroscopic to the more microscopic approach in the study of human injury. The examples cited herein are for illustrative purposes and for expediency are taken from our work at the University of Pennsylvania. As such, they deal primarily with neural and vascular tissue studies and relate to our specific interest in central nervous system trauma.

The diagram shown in Figure 1. is intended to depict the process where the level of mechanical loading is first related to the tissue deformation through the use of physical or mathematical models. This deformation is then used as the stimulus to investigate the response of the living tissue or single cells. Studies such as these may then lead to an improved understanding of tissue failure criteria and new avenues to address the issues of theraputic intervention and rehabilitation.

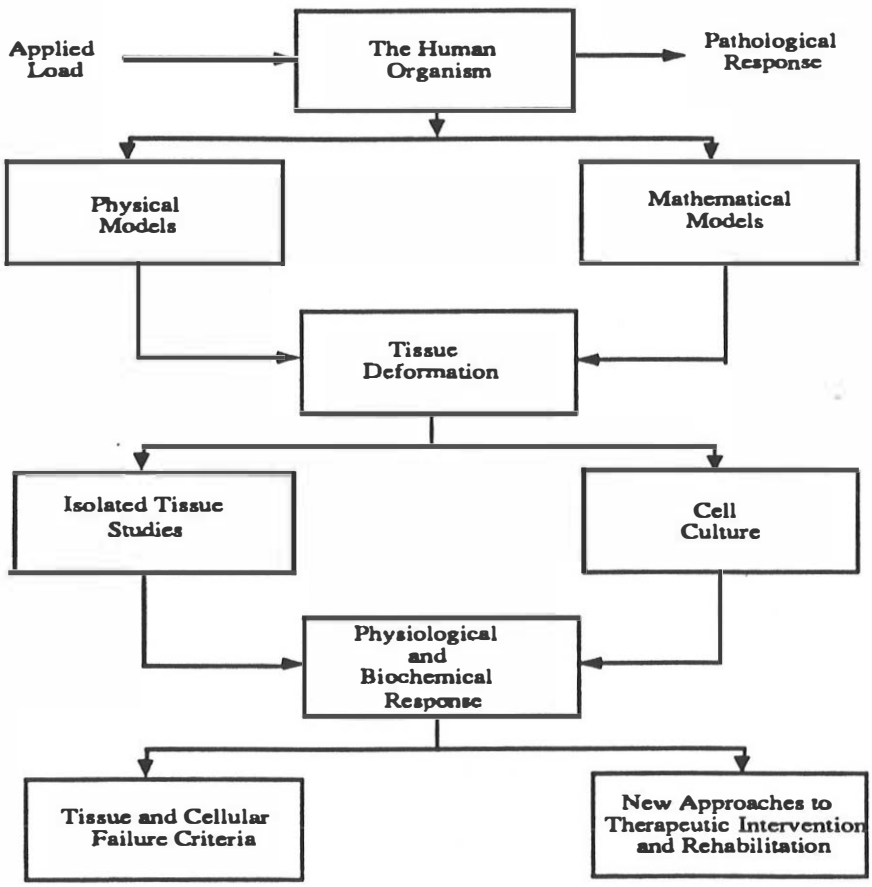

Figure 1

Transforming the Macroscopic Loads to Organ, Tissue, and Cellular Deformations

Central nervous system (CNS) trauma in general and brain injury in particular has been the subject of intensive biomechanics investigation for the past five decades. Therefore, CNS trauma will be the example that is used to demonstrate the concepts of transition from the macroscopic to the microscopic level of biomechanics research. Some of the earliest studies (1-4) suggested that the translational and rotational accelerations of the head serve as a macroscopic descriptor and predictive index with regard to the incidence of brain injury. Subsequent investigations, ranging from human volunteer experiments to animal model studies, (5-8) confirmed that inertial loading, its magnitude, duration, and direction relative to the anatomy can produce a broad spectrum of neuropathological findings. These various forms of injury to the brain include the following: cerebral concussion, cortical contusion, focal intracerebral hematoma, subdural hematoma, and diffuse axonal injury with prolonged coma. Each of these pathologic entities is distinctive and represents the structural or functional failure of the discrete elements within the brain.

It is reasonable to imagine that the deformations of the neural and neuraovascular elements within the brain vary in magnitude and topographic distribution as some complex function of the loading conditions, geometry of the brain and skull, and the constitutive properties of the tissue. Attempts have been made to measure the in-situ deformations (9-11) but the experimental difficulties have thusfar prevented any detailed information from being obtained. Because these data are so important in providing insight into the mechanisms of injury other approaches have been employed. These methods enable one to estimate the field parameters under dynamic loading ocnditions and they fall into two categories:

Physical Models- these devices are designed as surrogates for the anatomic structures of interest and have been used extensively in experimental mechanics to estimate local stress and strain;

Computational Simulations- analytical and numerical methods are employed to predict the detailed deformations of a structure under load.

Each of these methods has the limitation that they represent only an approximation of the actual anatomic structure. In the case of the skull and brain for example, analytical models are constrained to use simple two and three dimensional approximations for the geometry such as circular cylindrical, spherical, or ellipsoidal structures. The constitutive properties of the tissue must by necessity be modeled in a manner that may oversimplify the problem. Finite element methods on the other hand are potentially capable of the more complex analysis. Numerical schemes have been developed which permit one to incorporate the non-linear geometry of the structure and to accomodate a complete hiearchy of constiuttive expressions for the material.

Physical models have been a critical component of mechanics research in that theoretical representations at the very least need experimental validation and experimental stress and strain analysis is a well developed tool that has independently contributed to our knowledge of structural mechanics. The advantages of physical models relate to the fact that they are designed by the investigator. They are fabricated of synthetic materials that are selected by the designer to facilitate the measurements and they can be thoroughly instrumented as desired.

To gain further insight into the biomechanics of head injury, it is important to clarify the response of the brain tissue to the range of mechanical loads believed to cause injury. Physical models can be used to relate the loading kinematics of controlled animal experiments to the resulting injury pathology by estimating the deformation field. In 1943, Holbourn quantified the strain distribution of a surrogate brain material during a controlled applied load [12]. Sagittal, coronal, and horizontal sections of wax skulls were filled with

a 5% gelatin solution that closely represented the mechanical properties of brain tissue. While the skull was subjected to rotational loads, the photoelastic stresses within the material were mapped. Holbourn found that very high strain rates were produced in the superior margin of the brain in the sagittal model, the same region where an acute subdural hematoma occurs.

Holbourn used these results to postulate that a majority of the head injuries seen clinically were due solely to rotations of the head. Previously, many investigators had believed that a majority of injuries were produced primarily by the loose brain colliding against the rigid skull during impact loading. Holbourn suggested that injury resulted not from compression of the tissue components under such conditions, but rather from the shear strain induced in the brain tissue and neurovasculature under rotational loading conditions. This hypothesis was later confirmed by studies performed on a range of subprimates which showed that an array of head injuries (e.g. acute subdural hematoma, concussion, and diffuse axonal injury) could be produced using non-impact, angular acceleration (13-15). These animal experiments and the physical model studies by Holbourn established rotational loading as an important cause of head injury.

Despite the suggestion that rotational loads are an important cause of head injury, most of the subsequent physical models were subjected to non-rotational impact loading. More recently, however, Thibault et al constructed physical models of the baboon brain, subjected them to sudden rotational loads, and compared the spatial distribution of measured strain in the surrogate brain to pathological data from primate head injury experiments (16). Later, Margulies used physical models to investigate another type of head trauma (diffuse axonal injury) and to suggest a tolerance level for the onset of severe diffuse axonal injury in the baboon and adult human (17-18) Physical models can be used to measure how the strain response of the model is affected by changing the model geometry. The results from such an effort can be used to develop a scaling relationship that can be applied to a range of brain sizes. This scaling information can then be used to develop human injury tolerance levels.

Physical modeling can also be used to measure the changes that occur in brain deformation when brain tissue flows from the cranial vault during loading. During the course of dynamic loading, the regional rise in intracranial pressure causes brain material to flow through the foramen magnum at the base of the skull. Thus, the brain volume does not remain constant but decreases during the loading period thereby producing an "effective compressibility". However, the effect this exit of brain material has on the strain patterns in the brain remains unclear. Researchers have developed finite element models of the head that incorporate time-independent compressible material elements to simulate the exit of material, varying the value of the compressibility to fit physical model experimental data (19-20) Without experimental validation of the effect of this material compressibility on the strain field, however, problems may arise when using these finite element models to extrapolate the response of the head under conditions for which no experimental results from physical models exist. Testing physical models with variable effective compressibility will determine the extent such changes have on the strain pattern.

A device that has been used to accelerate the physical models was also employed successfully in previous animal and physical modeling experiments in our laborarory. The system consists of a six-inch Bendix HYGE actuator and linkage assembly which delivers a distributed inertial load to the primate head or physical model (Figure 2). Amplitude of the peak acceleration and pulse duration can be controlled by adjusting the set pressure applied to the cylinder, while acceleration waveshape can be changed by altering the geometry of the metering pin.A more detailed description of the HYGE device can be found elsewhere (16-17). An accelerometer (Endevco Instruments, San Juan Capistrano, CA) is mounted on the mechanical linkage arm and provides the loading data under these controlled kinematical conditions.

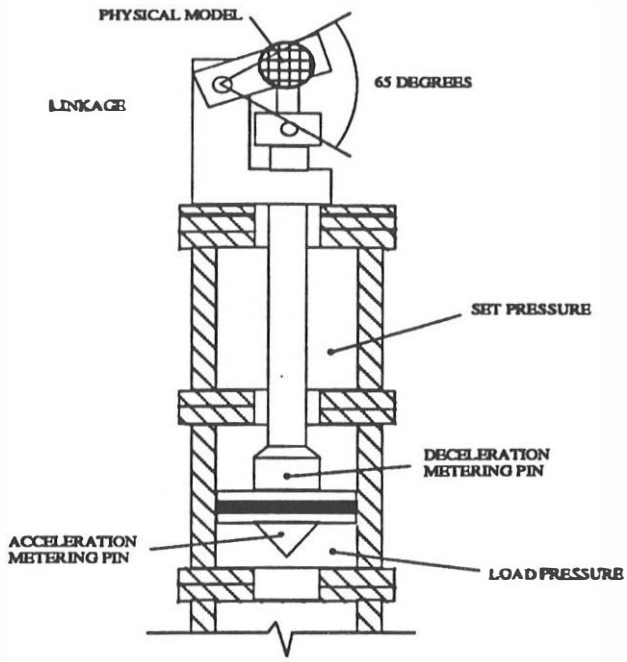

Figure 2

The physical models used in previous investigations by Thibault et al and Margulies (16-17) are described elsewhere. Various idealized geometries (including cylinders and hemicylinders), baboon skulls and three types of human skulls (neonatal, pediatric, and adult) (Carolina Biological Supply) have been subjected to controlled inertial loading. These skull models are prepared as hemisections and an example of a sagittal plane model is shown in figure 3. In this particular example the skull was cut 1.0 to 1.5 cm lateral to the sagittal midline and was manufactured to facilitate the insertion of a surrogate spinal column. The intended use of this particular model was to investigate the superior margin strains as they may serve to estimate the degre to which the parasagittal bridging veins are stretched. The distal end of the spinal column was fitted with a removable plate, permitting one to vary the membrane across the distal end, thereby changing the effective compressibility of the material (21).

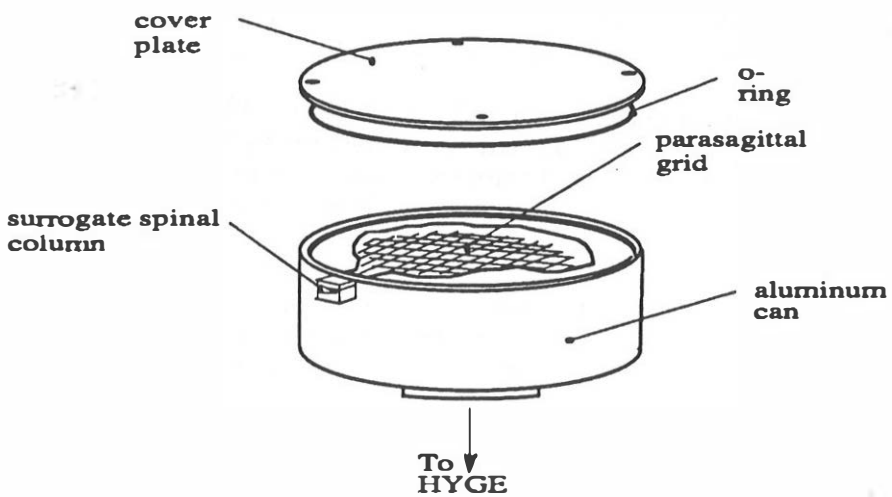

Figure 3

Presented in figure 4 is an example of a computation for a grid element located in the central region of the superior margin. This type of data will be used later to develop experiment parameters for stimulating isolated tissue and cell culture models. However, the data can be used independently to validate analytical and numerical simulations or to develop empirical scaling relationships that may be important in and of themselves for the purpose of scaling animal model studies to man.

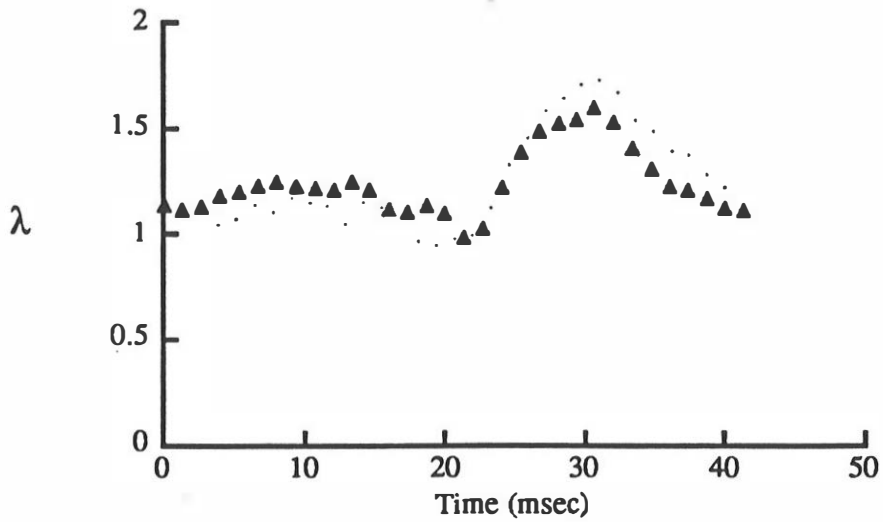

Figure 4

Mathematical models of head injury facilitate the study of the spatial and temporal responses of the brain structure across a broad range of inputs, whereas physical models are confined to discrete load levels dictated by the limits of the equipment. Bycroft, and Lee and Advani developed the first analytical model for head injury caused by rotational loads (22-23). They applied a symmetric torsional acceleration to an elastic sphere, and transformed the solution to a viscoelastic solution using the correspondence principle . The analytical solution showed that large shear strains could be generated in the region of the brain stem.

Liu and Chandran modeled the brain as an elastic sphere encased in a rigid spherical shell (24). Subjecting the model to rotational acceleration produced high stresses in the cortical and subcortical regions, indicating that rotational loads could produce injuries such as gliding contusions and subdural hematomas. Subsequent models of the same geometry, subjected to other loading conditions displayed the ability of the models to predict a threshold for concussion. In the process it drew attention to the the dependency of these injury levels on the mechanical properties of brain tissue.

Ljung developed viscoelastic models of different geometries (infinitely long cylinder, cylinder with one closed end, and a sphere) and placed a special emphasis on deformation in the superior sagittal sinus (25). Misra extended the geometric analysis by studying a prolate spheroid filled with a Kelvin material and subjected it to an angular acceleration pulse (26). Misra concluded that geometry may well have an important influence on the spatial and temporal distribution of strain, especially in the cortical and subcortical areas. Margulies investigated the strains deep within the white matter of a viscoelastic cylindrical model and compaired her results with physical model simulations

and the pathology of subhuman primate studies where the rotational accelerations in the coronal plane resulted in diffuse axonal injury with prolonged coma (27). Meaney conducted a similar injury-specific analysis of a viscoelastic structure designed to simulate the sagittal plane of the brain and focused on the superior margin strains. His model was used in concert with physical model studies and isolated tissue experiments to determine the threshold levels of inertial loading that are responsible for acute subdural hematoma (21). His numerical computations are depicted in figure 5.

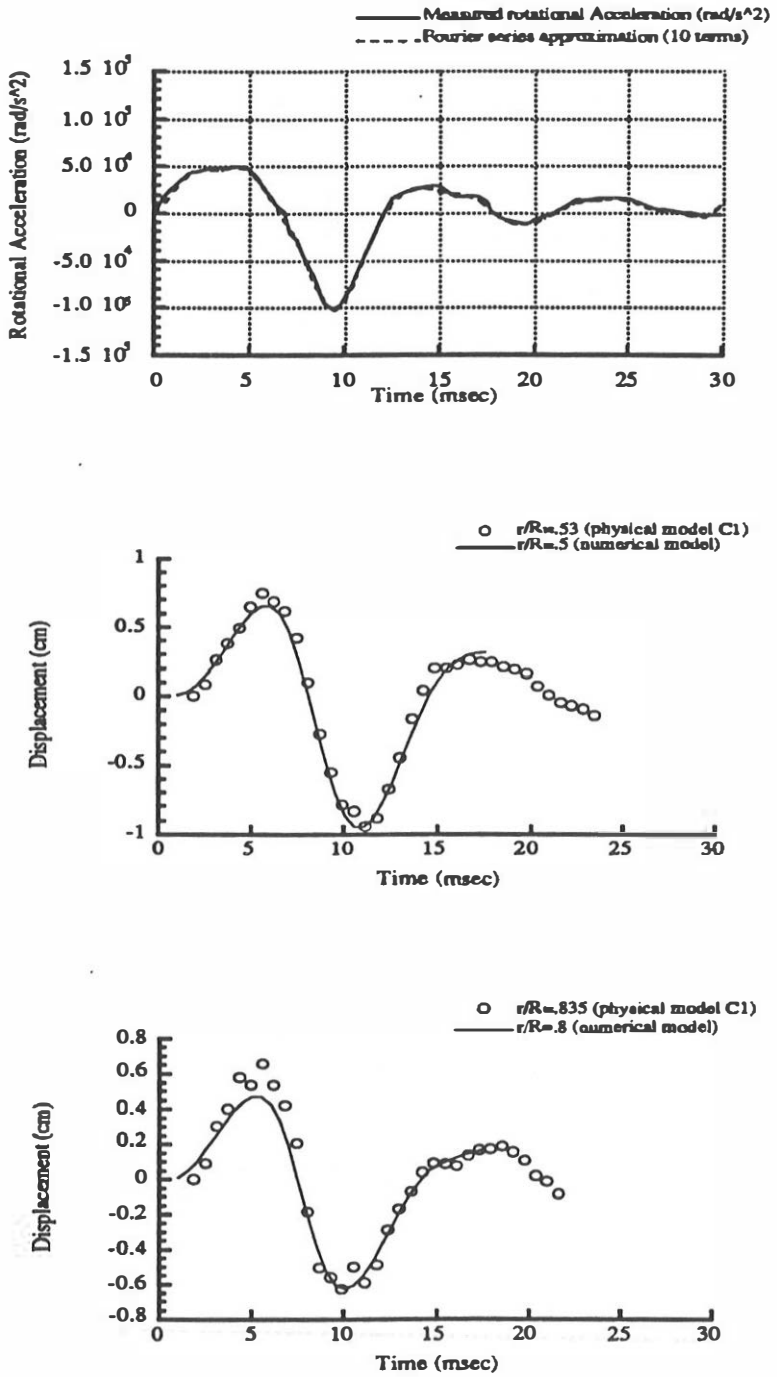

Figure 5

Shown in this figure is a Fourier series approximation of the inertial load compared with the actual forcing function of the experiment. This series approximation was used to drive the model. Subsequently one can see the comparison of the numerical estimation of the the deformation at various locations within the simulation and the actual experimental data obtained from the physical model study. This interplay between the computational simulations and experimental data from physical model studies is important if we are to have reasonable confidence in this research endeavor

In recent years the use of finite element methods to investigate the structural response of the brain to inertial loading has become a potentially important adjunct to experimental and analytical methods. In this past decade finite element programs have been used to investigate the structural response of the brain to inertial loading. Khalil and Viano (20a) reviewed the early use of such computational methods and their review is recommended by this author as supplemental reading. Linear analysis approaches have been used by investigators in order to estimate the deformations that occur wihtin the brain under dynamic loading conditions (20b) these estimates are restricted in that the deformations and rotations of the structure are assumed to be small. More recently, software has become available that permits the investigator to analyze large deformation problems with a comprehensive hierarchy of constitutive expressions for the materials. Programs such as DYNA have been used by a number of researchers (20c) . Their simulations require a detailed knowledge of the geometry of the structure and the constitutive properties of the brain material, but they are not restricted to the small deformation assumptions of previous numerical schemes. Most recently a simulation using this approach was conducted and compared to the results of the physical model studies that were discussed earlier with favorable agreement (21). Again, it is our belief that this interaction between the experimental and computational approaches in biomechanics is prudent.

Experimental Methodologies to Investigate the Response of Isolated Tissue and Cell Culture Models to Controlled Mechanical Stimulation

Based upon the previous discussion, the neural and neuro- vascular elements of the central nervous system experience deformations that can result in a continuum of injury response in the sense that there are levels of strain that produce no response, spontaneously reversible forms of trauma, and irreversible injury and cell death. If the physical and mathematical models can help us to estimate the deformations experienced by the components of the central nervous system then it is reasonable to explore methods of subjecting isolated tissue elements or single cells to controlled mechanical stimulation. This section is an attempt to answer the following questions in this regard:

1. Can we develop the experimental methods that enable us to deform tissue or cells in culture in a controlled and reproducible manner?
2. Can we measure the load deformation characteristics of the living material?
3. Is it possible to examine the physiological response at the tissue and cellular level to dynamic mechanical stimulation in a way that may shed light upon tolerance criteria and detailed mechanisms of injury?

Researchers in our lab and others have examined the role of mechanical forces in the etiology of head injury by observing the response of an isolated unmyelinated axon to rapid elongation(28-29). A graded depolarization in response to increasing levels of strain and strain rate in the squid giant axon has been observed. This graded response suggests a spectrum of injury severity for individual axons, ranging from mild, reversible injury for stretch ratios less than or equal to 1.10 to permanent deficit at 1.20 and structural failure at 1.25 which will be discussed later. Diffuse axonal injury (DAI) observed in a subhuman primate model appears morphologically as microscopic abnormalities distributed throughout the white matter, independent of any focal injury (14,30,31). It would be of great interest to understand this abnormality and it may be possible to conduct such studies

on the isolated axon. One feature of the axonal damage observed is abnormally shaped nodes of Ranvier, structures unique to myelinated nerves. In addition, the variation in the mechanical structure between the node and internode suggests that strains may not be distributed uniformly along the myelinated fiber as is assumed for the unmyelinated axon. Thibault et al. dynamically stretched frog sciatic nerve bundles, a myelinated nerve preparation, and measured the compound action potential as an indicator of functional viability (32). Response to injury varied from a transient alteration in the signal with small stretch to an irreversible change in the compound action potential following a large stretch. Gennarelli et al. demonstrated that dynamic elongation of guinea pig optic nerves resulted in axonal damage similar to that seen morphologically in cases of human DAI (33). While these studies suggest functional and structural changes of myelinated nerves as a result of dynamic stretch, mechanically loading a nerve bundle does not result in a reproducible, quantifiable load on each axon. The responses of many axons are measured, leading to a final correlation between some 'average' response and the overall or 'average' load. Using a single myelinated nerve fiber, on the other hand, allows for the measurement of an individual axon response to a known loading condition. Gray and Ritchie demonstrated functional changes, including reversible conduction block and altered action current, in a single myelinated frog axon due to static stretch (34) However, when the axon was stretched 5% in less than one millisecond, no consistent change in potential was measured. The lack of single fiber response to dynamic injury in Gray and Ritchie's experiment is likely due to two factors. First, applying a 5% stretch to the portions of the bundle nearest the dissected single fiber does not translate directly to a 5% fiber stretch because the single fiber may slip within the bundle. More importantly, a 5% stretch may be too small to elicit an injury response. Data from Galbraith's dynamic elongation experiments on squid axons indicates only a small transient depolarization in response to a 5% stretch (29). Therefore, the response of a single myelinated nerve fiber to larger dynamic strains still needs to be studied before conclusions can be drawn concerning the consequences of dynamic stretch injury.

In addition to investigating the response of the neural tissue we have been studying the effects of mechanical stimulation on blood vessel specimens. Our animal model data suggest that a myogenic response to mechanical stimulation can result in a vasospasm with the associated alterations in blood flow and metabolism. Because of the cylindrical nature and the relatively small sizes of the axons and vessels miniature material testing machines have been developed and are integrated onto a microscope stage. This approach is shown schematically in Figure 6.

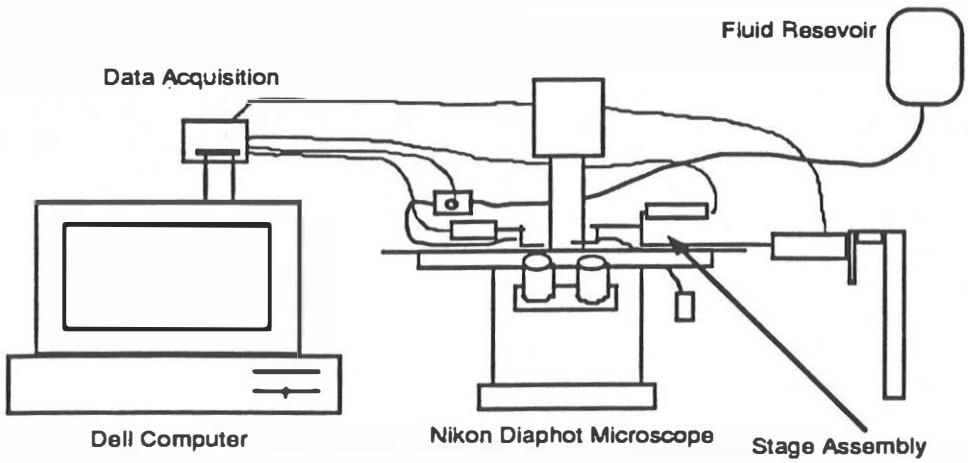

Figure 6

Both single axons and isolated blood vessels have been used in these systems to measure the mechanical stimuli and the biological response. In the case of the axons measurements of membrane potential, voltage clamp current and cytosolic free calcium concentration have been made. In the case of the isolated blood vessels we have recorded on video tape a spontaneous contraction of the vessel in response to high strain rate uniaxial loading.

In addition to the methods described which were designed to subject islated axons and blood vessels to controlled mechanical stimulation, we have developed techniques to apply loads to cells in culture.

This cell culture system permits one to investigate the effects of mechanical deformation on neural and vascular tissue physiology, morphology and biochemistry. Cells are grown on a transparent, circularly-clamped, elastomeric substrate which is deflected into a spherical cap by a uniform pressure applied to the underside of the substrate. The resulting biaxial tension in the substrate creates a state of biaxial strain in the attached monolayer of cells. Presumably, the deformation response of a cell to substrate extension depends upon its attachments and its structure; consequently, it is important to determine cell strain in each preparation studied.

Nevertheless, it is possible to subject a population of cells to dynamic biaxial extension and to measure the biological response to such stimulation.

Thusfar, we have described the mechanical methodologies to stimulate the tissue or cells in culture. It remains to describe the techniques that are currently being used to assess the biochemical and physiological consequences of mechanical stimulation.

It is important to first note that my colleagues and I have placed particular emphasis upon the role of calcium in mediating the physiological response of cells in the injury process. Therefore, we have gained most of our experience in this area of cellular biomechanics and the injury process by evaluating changes in intracellular calcium in response to mechanical trauma.

Functional Response of Tissue and Cell Culture Models to Mechanical Injury

Calcium is a likely candidate to play a role in the cell's injury response as the importance of calcium in normal cell function is well established and abnormal levels of intracellular calcium are known to be damaging to cellular components. Calcium is essential in maintaining the structural integrity and the normal function of nervous tissue (35-36). Cell injury can occur when an external stimulus damages the cell membrane thereby impairing its ability to act as a barrier to extracellular calcium. The resulting increased calcium influx can overwhelm the cellular mechanisms that normally maintain a low, relatively constant intracellular calcium concentration (37-38). If the cell is unable to sequester or expel sufficient calcium, the cytosolic free calcium level may surpass a critical threshold, triggering a series of pathological events. For instance, the disassembly of microtubules begins at calcium concentrations above 10 micromolar and is greatly accelerated at millimolar concentrations (36) Neurofilament degradation by calcium-activated neutral proteases begins when calcium concentrations reach 50-100 micromolar (39-40). These disrupted cytoskeletal elements, unable to diffuse across the membrane, may lead to an osmotic pressure gradient and subsequent swelling. In a nerve fiber, the accumulation of intracellular debris may occur at or near the nodes of Ranvier where the axon diameter changes significantly. Jones and Cavanagh demonstrated that, for neurofilament degradation induced chemically over a period of weeks, paranodal or nodal swelling occurred due to the accumulation of filamentous masses in myelinated peripheral nerves (41). Increased calcium influx following membrane damage has other consequences. Variations in intracellular calcium can disrupt normal axon functions, such

as axoplasmic transport. Ochs et al. found that exposing a desheathed nerve to 25-100 mM extracellular calcium resulted in blocked axoplasmic transport after about two hours, probably due to microtubule depolymerization (35). In addition, efforts to maintain low intracellular calcium by sequestration or extrusion may lead to diminished mitochondrial function and metabolic depletion of the cell (39-37). This sequence of events leading to cell injury or death - - altered membrane permeability or membrane damage, calcium influx, structural disruption - - has been hypothesized for cells in general that are exposed to biochemical agents that alter the cell membrane. Balentine observed that the sequelae of spinal cord impact injury, disruption of the myelin and granular dissolution of the axoplasm, were likely a result of increased intracellular calcium. The mechanism by which the impact injury caused an elevated calcium concentration, however, was not addressed.

In our work, it has been hypothesized that dynamic mechanical elongation of a nerve fiber creates transient membrane defects or "pores" which effectively increase membrane permeability and allow a damaging influx of calcium. Intracellular calcium transients resulting from the rapid mechanical deformation of cells have been demonstrated by other researchers in this lab. Using the fluorescent calcium indicator dye, Quin2, Winston recorded elevated calcium levels in endothelial cells attached to a biaxially strained substrate and demonstrated the cells' ability to recover to resting calcium concentration (42). Using a similar technique, cytosolic free calcium transients were measured in vascular smooth muscle cells (43). In the unmyelinated squid giant axon, an increased intracellular calcium concentration in response to a dynamic uniaxial elongation was measured with an ion-selective internal microelectrode (44). The calcium transients for several levels of stretch will be discussed later in the chapter. For a stretch ratio less than or equal to 1.1, the giant axon spontaneously recovered to its resting calcium concentration. Above this level of stretch, however, the intracellular calcium concentration remained abnormally high or increased to the calcium concentration in the external bath.

Measurements of intracellular free calcium transients following stretch injury are made using the fluorescent calcium indicator dye, fura-2 (Molecular Probes, Inc.). The lipid soluble form of the dye, fura-2/AM, diffuses across the axolemma. Once in the axoplasm, the acetoxy-methyl ester is cleaved from the dye molecule by endogenous esterases, leaving fura-2 free acid which binds ionic calcium. Upon binding calcium, the excitation spectrum for the fluorescent dye shifts (46). The maximum fluorescence of unbound fura-2 occurs at about 360 nm wavelength excitation while the peak for Ca^{2+}-bound dye is close to 340 nm (46-47). Therefore, the intensity of the emitted fluorescence at two wavelengths yields a relative measure of the amount of bound and unbound dye in the cell. A ratio of these measurements is used to calculate the intracellular free calcium concentration.

The shift in the fluorescence maximum upon binding Ca^{++} can be exploited by using two excitation wavelengths, one near the Ca^{++}-saturated maximum and the other near the Ca^{++}- free maximum. If the concentrations of free and bound dye are sufficiently dilute that the fluorescence of each species is proportional to its concentration, then the fluorescence intensity at the two excitation wavelengths is given by:

$$\begin{aligned} F_1 &= S_{f1}C_f + S_{b1}C_b \\ F_2 &= S_{f2}C_f + S_{b2}C_b \end{aligned} \qquad (1)$$

where C_f is the concentration of free Fura-2, C_b is the concentration of Ca^{++}-bound Fura-2, and the S's are proportionality constants. Since Ca^{++} and Fura-2 form a 1:1 complex, C_f and C_b are related by

$$C_b = \frac{C_f[Ca^{++}]}{K_d} \qquad (2)$$

where K_d is the dissociation constant. Substituting (2) into (1) and taking the ratio $R = F_1/F_2$ yields an equation for the calcium ion concentration:

$$[Ca^{++}] = K_d \frac{R-R_{min}}{R_{max}-R}\left(\frac{S_{f2}}{S_{b2}}\right) \qquad (3)$$

where R_{min} is the fluorescence ratio with zero calcium (S_{f1}/S_{f2}) and R_{max} is the ratio at calcium saturation (S_{b1}/S_{b2}). It is important to note that the calculated calcium concentration is independent of the dye concentration. This will make the calcium measurement insensitive to variations in the amount of dye loaded between different experiments and variations of absolute fluorescence due to photobleaching during the course of one experiment. However, any autofluorescence must be subtracted before the ratio is taken.
Both isolated single axons and neural and vascular cells in culture were studied using this intracellular indicator with a system depicted in figure 7.

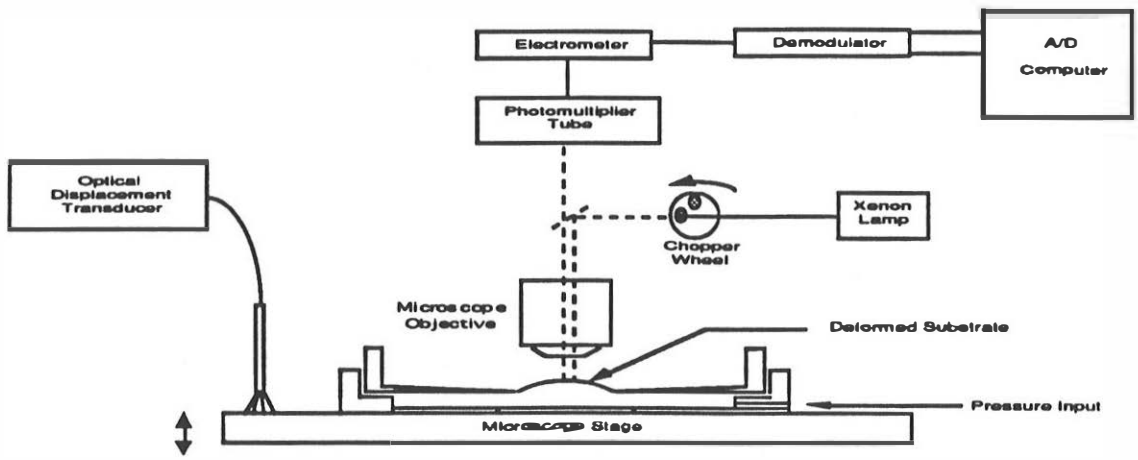

Figure 7

Figure 8 depicts three experiments using the calcium sensitive fluorescant indicator dye, Quin 2. Figure 8 A shows the response of endothelials cells to a stretch of approximately 8% at a strain rate of 10 sec^{-1}. Current from the photomultiplier tube is proportional to calcium concentration in the cytosol. Figure 8 B shows a series of six identical stimuli which were delivered to cell following exposure to a 0.1% gluteraldehyde solution. Each stimulus was delivered at one minute intervals and the figures are plotted on the same graph for convenience. One can follow the accumulation of calcium and the ultimate death of the cell. Trypan blue stain was used to confirm the observation. Figure 8 C demonstrates the spontaneous accumulation of calcium following a traumatic level of cell deformation.

Vascular smooth muscle and neural cells in culture have exhibited a similar response to mechanical stimulation. Isolated tissue elements such as the squid giant axon

and the single myelinated fiber from the frog sciatic nerve have demonstrated functional changes as measured by the resting membrane potential as can be seen in Figure 9. This series of studies was conducted using the squid giant axon. For increasing levels of stretch at high strain rates the axon depolarizes to levels that are exponentially dependent upon the mechanical stimulus. Clearly it is possible to controllably deform isolated tissue elements and cells in culture, and to measure the electrical and chemical changes that may be elicited by the mechanical stimulus. These tools extend our capabilities in the context of injury biomechanics by providing opportunities to investigate the effects of mechanical deformation on the living elements that constitute the organs and organisms when these structures are subjected to forces from the external environment.

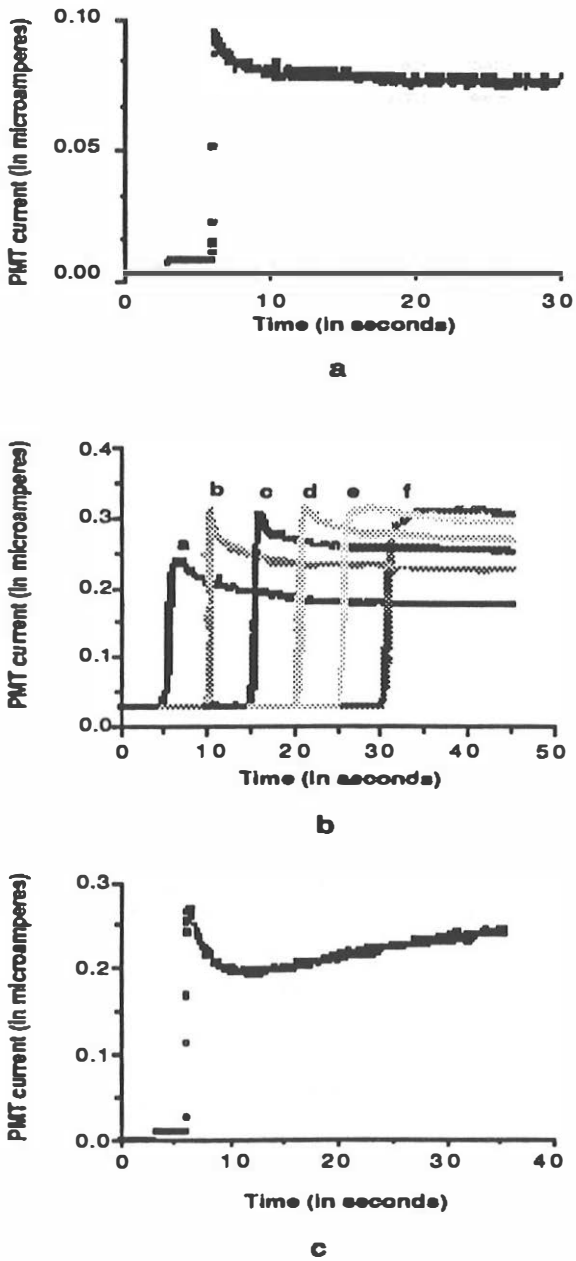

Figure 8

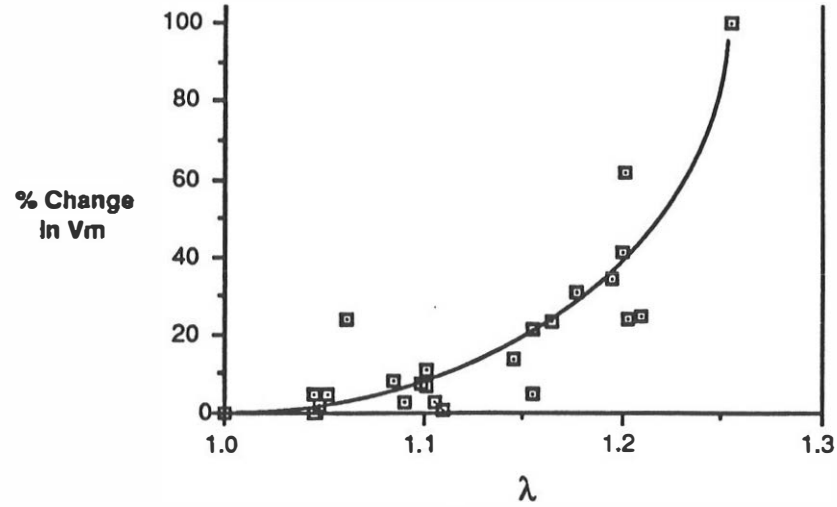

Figure9

Analysis of the Mechanisms of Cell Injury

It is this topic area that may serve to bring together the molecular biology and the biomechanics communities that have a common interest in understanding the mechanisms of injury to the cell. At this level the biomechanician is challenged by the structural complexity of the cell, its transport mechanisms and the myriad of biochemical processes that are potentially influenced by the state of stress or strain that the cell structure may endure.

The mechanism by which dynamic elongation initiates the injury sequence is hypothesized to be a stretch-induced transient change in membrane permeability. In 1981, Ganot et al. reported increased membrane conductance in the *Myxicola* giant axon in response to a rapid transverse mechanical stimulus (48). The reversal potential of the mechanically altered conductance for small stimuli was very close to that of the leak conductance, suggesting a similarity between these two pathways. A mechanically-induced conductance increase in a biological membrane was also described by Terakawa and Watanabe (49). Slow injection of a small fluid volume into a squid giant axon produced a hyperpolarization and increased membrane conductance, perhaps as a result of increased potassium or leak conductance.

Using a model cell membrane consisting of lipid bilayer and gramicidin channels, Hunter measured membrane conductance in response to biaxial strain at various strain rates (50). Although gramicidin channel conductance was not strain dependent, increased membrane conductance with strain was measured for bilayers containing no gramicidin that had an initial, unstressed conductance of greater than 3×10^6 pS/cm^2. Hunter hypothesized that these bilayers contained microscopic defects that allowed increased conductance with dynamic membrane strain.

The above studies have demonstrated changes in biological membrane conductance as a function of mechanical deformation. These conductance changes need to be related to the physiologic consequences of stretch injury to form a coherent injury hypothesis. In our research, strain-dependent membrane conductance and accompanying changes in ion transport have been modeled in order to develop an analytical expression describing the experimental stretch-induced calcium transients.

An analytical model is being developed to describe the change in calcium permeability of the nodal membrane as a function of applied strain. In this model, the membrane is treated as a viscoelastic matrix material containing cylindrical elastic inclusions

representing membrane proteins. Applying a dynamic tensile strain to the nerve fiber deforms the nodal membrane where local stress concentrations develop at the inclusion-matrix interface, leading to the formation of transient defects or "pores". These defects in the membrane cause an increase in non-specific leak conductance, allowing calcium to diffuse down its concentration gradient into the axoplasm. From measurements of nodal displacement during dynamic stretch of a single myelinated axon, as described previously, a transfer function for nodal strain resulting from fiber strain will be established.

Calculation of the inclusion-matrix interface stress concentration due to an applied strain is based on Hashin's formulation of the inclusion problem (51). Hashin solves the problem of an isotropic elastic spherical inclusion imbedded in an infinite three-dimensional isotropic elastic matrix. Using the correspondence principle and geometrical modifications, Hashin's analysis will be applied to the case of an isotropic linearly elastic cylindrical inclusion in an isotropic viscoelastic matrix.

An expression for the diffusivity of calcium ions in the membrane, taking into account the hindered diffusion through membrane pores, will be developed using pore theory. As a first approximation, the membrane defects will be considered right cylindrical pores of length l, equal to the thickness of the membrane, and radius r(t), as shown in Figure 10. The time varying function for the pore radius will be chosen considering the stress concentration calculations described above and data in the literature on lipid-protein interactions. To simplify the analysis, electrical interactions between solute molecules and between solute molecules and the pore walls are neglected. Calcium ions are assumed to be rigid spheres of radius a, calculated from the Stokes - Einstein relation:

$$a = \frac{R\,T}{6\,\pi\,\eta\,D\,N},$$

where R = gas constant, T = absolute temperature, h = solution viscosity, D = free diffusion coefficient of molecule, and N = Avogadro's number [45].

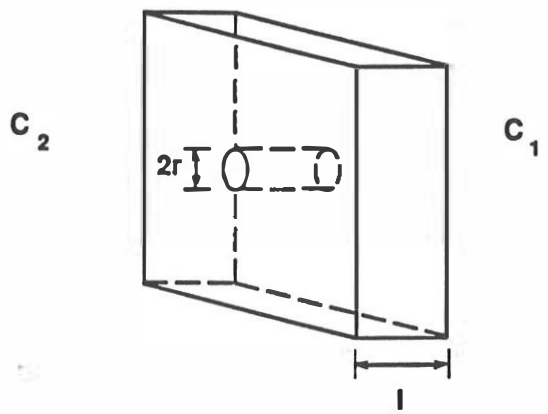

Figure 20

The diffusivity of calcium ions in the membrane is decreased from that in free solution by two factors: steric hindrance at the entrance to the pore, and friction between the pore wall and diffusing molecule. In order to enter the pore, the center of a diffusing molecule of radius a must pass through the central region of the pore swept out by a radius of r(t)-a so as not to collide with the pore edge (52). Therefore, the relative area for diffusion can be expressed as a ratio of this area available to the molecule to the actual pore area. That is,

$$\frac{A(t)}{A_o(t)} = \frac{\pi\,[\,r(t) - a]^2}{\pi\,r^2(t)} = \left(1 - \frac{a}{r(t)}\right)^2,$$

where if a<<r, A/A_o approaches one, corresponding to free diffusion (53). If a=r, A/A_o will equal zero, and the molecule will be sterically excluded from the pore.

The fractional decrease in diffusivity due to friction between the molecule and the pore wall can be calculated using :

$$\frac{f_o}{f(t)} = 1 - 2.104\,\frac{a}{r(t)} + 2.09\left[\frac{a}{r(t)}\right]^3 - 0.95\left[\frac{a}{r(t)}\right]^5,$$

where f_o corresponds to the frictional drag on the freely diffusing molecule (i.e. a<<r). Combining these two effects to obtain an expression for the hindered diffusivity of the molecule in the membrane results in creates transient membrane pores, the pore radius is proportional to the stretch ratio for a uniaxial elongation such as that applied to the squid axon. This assumes that increasing the level of strain does not solely increase the number of pores in the membrane. Furthermore, assuming the permeability of the axolemma to calcium is determined by the hindered diffusivity of calcium in the membrane (see below), the flux of calcium into the axoplasm, and thus the peak intracellular calcium concentration, is proportional to the strain dependent calcium diffusivity. This proportionality is, of course, complicated by the sequestration of calcium into intracellular stores. However, that the data in Figure 11 exhibits a trend similar to the relative diffusivity curve of Figure 12 suggests that pore theory is an appropriate choice for the analysis of stretch-induced calcium transients.

$$D_m(t) = D_{free}\left(1 - \frac{a}{r(t)}\right)^2\left(1 - 2.104\,\frac{a}{r(t)} + 2.09\left[\frac{a}{r(t)}\right]^3 - 0.95\left[\frac{a}{r(t)}\right]^5\right).$$

The relative diffusivity, or $D_m(t) / D_{free}$, is plotted in Figure 12.

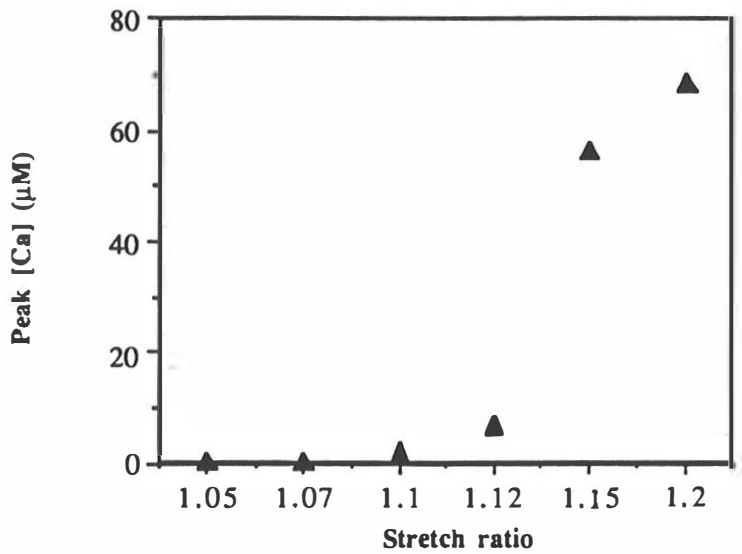

Figure 11

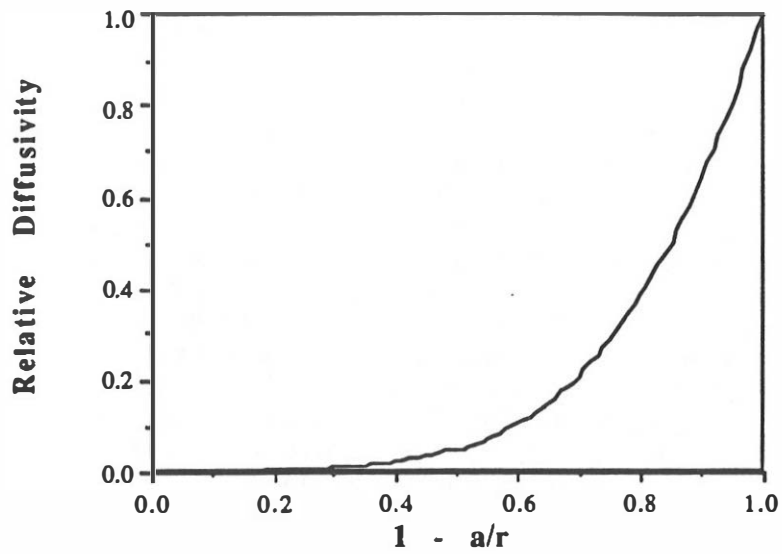

Figure 12

Considering the membrane a barrier of thickness l separating two solutions of constant calcium concentrations C_1 and C_2, as in Figure 12, the calcium flux can be written as,

$$J(t) = P(t)\,[C_2 - C_1]\,,$$

where J(t) is the diffusion flux across the membrane and P(t) is the permeability of the membrane to calcium. Assuming that diffusion of calcium through membrane pores is the primary determinant of membrane permeability to calcium,

$$P(t) = \frac{\alpha(t)\,D(t)}{l}\,,$$

where a(t) is the area fraction of pores in the membrane, and D(t) is the hindered calcium diffusivity calculated earlier. In this analysis, interaction between pores and end effects of the pores are neglected.

Flux experiments are being carried out in this lab to characterize the size of the strain-induced pores using radiolabeled ions of various radii. This data may provide a method to separate the effects of pore size and the number of pores, which together determine the flux.

It is hypothesized that the deformation of the cell's membranes causes an increse in permeability to ions due to the formation of defects or pores. This theory of mechanically-induced poration is supported by the observation that osmotically swelled red cells become permeable to the relatively large hemaglobin molecule (54). Furthermore, upon removal of the osmotic gradient , the membrane's integrity is restored. The red cell membrane is capable of only a 2-4% increase in in area before lysis occurs (54). Regions of high strain can recruit lipid from adjacent regions to relieve the strain. Therefore, the rate at which the strain is applied will determine the extent of the induced poration. Further, it is assumed that within limits, the pore formation is transient and reversible just as the red cell reseals when the distending pressure is removed.

Closure

With the exception of crush injury, the mechanical forces which lead to the central nervous system trauma are applied dynamically with a characteristic time course of 50 milliseconds or less. Little is known, however, regarding the time course of the pathophysiological response of the tissue. The models developed in our laboratory are designed to investigate the underlying mechanisms of injury, determine the threshold of mechanical stimuli that produces injury, and explore the time course of the pathophysiological events in order to define windows of opportunity and strategies for therapeutic intervention. The macroscopic analysis of central nervous system injury is complicated by the fact that the tissue or organ response is dictated by the cellular response. We are attempting to move biomechanics and injury research toward the areas of membrane mechanics, cytomechanics and transport process analysis at the cellular level.

In the past, we had used a primate model to replicate specific forms of injury. We focused our attention on Diffuse Axonal Injury (DAI) and Acute Subdural Hematoma (ASDH) because epidemiological data indicated that these forms of injury were responsible for approximately 70% of the mortality and morbidity associated with brain injury. By subjecting physical models or surrogates of the skull-brain structure to loading conditions which produced these discrete forms of brain injury in the primate model, we were able to estimate the magnitude and temporal nature of the deformations which were experienced by the various neural and neurovascular elements in association with these injuries. With this information, we developed a strategy to investigate the biomechanics of injury at the isolated tissue and cellular levels in order to begin to simplify this complex analysis. Accordingly, we designed instrumentation which permits the study of isolated axons, blood vessels and cells in culture under conditions of controlled mechanical deformation.Utilizing these technologies, we demonstrated that high strain rate deformation of the axolemma led to an elevated level of intracellular calcium.

Cell membrane ionic permeability is directly effected by high strain rate deformation which leads to an immediate elevation in cytosolic free calcium ion concentration. This traumatic rise in cytosolic free calcium in neurons has been implicated in cytoskeletal disruption, functional impairment, cell swelling, and ultimately cell death, while in smooth muscle cells the event can lead to spontaneous contraction. Neural tissue can respond by sequestering calcium or pumping it from the cytoplasm. However, the pumping mechanisms are dependent upon oxidative metabolism and may be compromised if blood flow to the tissue is reduced by vessel reactivity or structural failure.

Our current findings suggest that the cerebrovasculature responds to mechanical deformation under conditions of high strain rate loading. This response, in the form of a transient spasm, could result in regional reduction of cerebral blood flow. To investigate the mechanism of this mechanically-induced vasospasm, we return again to the cellular level and now focus on the smooth muscle element of the vessel wall. We have preliminary data demonstrating elevated levels of intracellular calcium in smooth muscle cells in culture. Transient changes in cytosolic free calcium can produce a spontaneous contraction and, on a more macroscopic level, can lead to vasospasm. We hypothesize that, in situ, these events occur in concert with the neural tissue insult as previously described.

Figure 13 demonstrates our current thinking with regard to the injury cascade that can occur as a direct result of dynamic elongation of the axon for example. This process will be exacerbated if their is an interruption in local blood flow accompanying the direct mechanical insult since the cell requires energy to actively pump calcium from the cytosol.

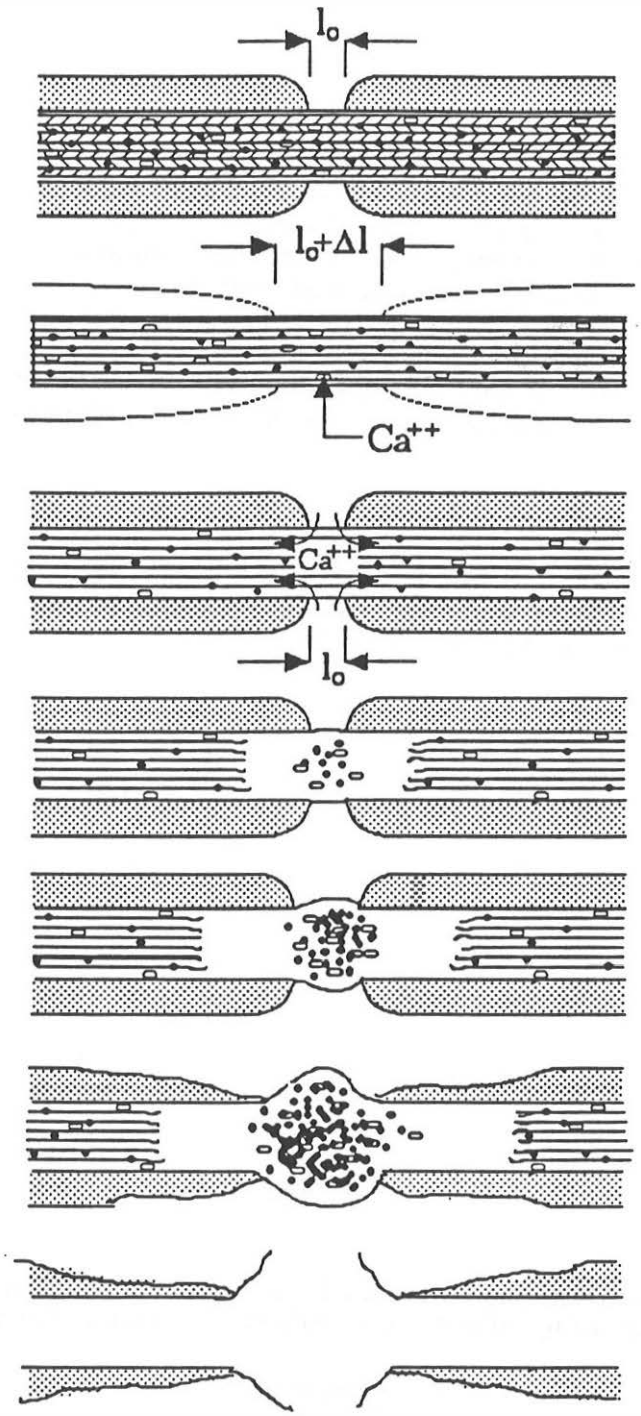

Resting Axon

Stimulus
Controlled Strain and Strain Rate

Elevated Intracellular Calcium

Excess Calcium produces CANP and Cytoskeletal Depolimerization

Accumulation of Vesicles and Elevated Protein Solution

Increased Osmotic Pressure with Cell Swelling

Elevated Intracellular Hydrostatic Pressure and Axolemma Rupture

Figure 13

Acknowledgements

I would like to take this opportunity to thank my former students Drs. Susan Margulies, James Galbraith, Flaura Winston, Catherine Hunter, David Meaney, Kenneth Barbee, and Robert Boock and Adam Landsman for it has been their hard work that has enabled us to move in this direction. My current students Katherine Saatman, Robert Cargill, Lynn Bilston, Daniel Goldstein, Kristen Belliar, Kristy Arbogast, and Michele LaPlaca are continuing this work.

I would also like to thank the National Institutes of Health, the National Highway Traffic Safety Administration, and the Centers for Disease Control for their support over these last ten years.

LITERATURE CITED

1. Gurdjian, E. S., H. R. Lissner and L. M. Patrick. Protection of the Head and Neck in Sports., J. Amer. Med. Assn. 182: 509-512, 1962.

2. Denny-Brown, D., Russell, W.R., Experimental cerebral concussion., Brain, 64:93-164, 1941

3. Holbourn, AHS, Mechanics of brain injuries., Brit. Med. Bul. **3**, pp. 147-9 1945

4. Ommaya A.K., Hirsch A.E., Flamm E.S. and Mahone R.H., Cerebral concussion in the monkey: an experimental model, Science, 153:211-212,1966.

6. Ommaya, A., Gennarelli, TA, Cerebral concussion and traumatic unconsciousness., Brain 97, pp. 633-654, 1974

7. Gennarelli, TA, Thibault, LE, Pathophysiologic responses of rotational and translational accelerations of the head., Proceedings of the 16th Stapp Car Crash Conference, SAE, pp. 296-308, 1972

8. Gennarelli, TA, Thibault, LE Bioemechanics of acute subdural hematoma. J Trauma **22**:8 pp. 680-696, 1982

9. Ommaya A.K., Hirsch A.E., and Martinez J.L., The role of whiplash in cerebral concussion, Proceedings of the 10th Stapp Car Crash Conference, November, 1966.

10. Shatsky, S, Alter, WA, Evans, DE Traumatic distortions of the primate head and chest: Correlation of biomechanical , radiological, and pathological data. Proceedings of the 18th Stapp Car Crash Conference, SAE, pp. 351-381, 1974

11. Prudenz, R, Sheldon, C, The lucite calvarium - a method for direct observation of the brain. II. Cranial trauma and brain movement., J Neurosurg, **3**: p487, 1946

12. Holbourn, A. H. Mechanics of Head Injuries. Lancet. 2: 438-441, 1943.

13. Abel, J., T. Gennarelli and H. Segawa. Incidence and severity of cerebral concussion in the rhesus monkey following sagittal plane acceleration., Proc. of the 22nd Stapp Car Crash Conf. SAE: 33-53, 1978.

14. Gennarelli, T., L. Thibault, J. Adams, D. Graham, C. Thompson and R. Marcinin. Diffuse axonal injury and prolonged coma in the primate., Ann. Neurol. 12: 564-574, 1982.

15. Gennarelli T.A., Ommaya A.K. and Thibault L.E., Comparison of translational and rotational head motions in experimental cerebral concussion, Proceedings of the 15th Stapp Car Crash Conference, November, 1971.

16. Thibault, L., A. Bianchi, J. Galbraith and T. Gennarelli. Analysis of the strains induced in physical models of the baboon brain undergoing inertial loading., Proc. of 35th ACEMB. 8, 1982.

17. Margulies, S. and L. Thibault. A proposed human tolerance criteria for diffuse axonal injury., J. Biomechanics. : (in press).

18. Margulies, SS, Thibault, LE, An analytical model of traumatic diffuse brain injury., J Biomech Eng, 111: pp. 241-249, 1989

19. Ward, CC, Thompson, RB, The development of a detailed finite element brain model., Proc of 19th Stapp Car Crash Conf, pp. 641-674, 1975

20. Lee, MC, Melvin, JW, Ueno, K, Finite element analysis of traumatic acute subdural hematoma., Proc. 31st Stapp Car Crash Conf., pp.67-77, 1987

20a. Khalil, TB, Viano, DC, Critical issues in finite element modeling of head impact., Proc. 26th Stapp Car Crash Conf, pp. 87-102

20b. Cheng, LY, Rifai, S, Khatua, T, Pziali, RL, Finite element analysis of diffuse axonal injury., Proc. of 33rd Stapp Car Crash Conf., 1989

20c. Tong, P, DiMasi, F., Carr, G, Galbraith, C, Eppinger, R, Marcus, J, Finite element modeling of head injury response to inertial loading., Proc. 12th Int. Tech. Conf. of Exp. Safety Vehicles, Gothenburg, Sweden

21. Meaney, DF, Biomechanics of acute subdural hematoma in the subhuman primate and man, Univ. of Pennsylvania Ph.D. dissertation, 1991

22. Lee, Y. C. and S. H. Advani. "Transient response of a Sphere to Torsional Loading - a Head Injury Model." Math. Biosciences. 6: 473-486, 1970

23. Bycroft, G. N. "Mathematical Model of Head Subjected to an Angular Acceleration." J. Biomech. 6: 487-495, 1973.

24. Liu, Y. K., K. B. Chandran and D. V. von Rosenburg. "Angular Acceleration of Viscoelastic (Kelvin) Material in a Rigid Speherical Shell - A Rotational Head Injury Model." J. Biomechanics. 8: 285-292, 1975.

25. Ljung, C. "A Model For Brain Deformation Due to Rotation of the Skull." J. Biomech. 8: 263-274, 1975.

26. Misra, J. C. and S. Chakravarty. "A Study on Rotational Brain Injury." J. Biomech. 17(7): 459-466, 1984.

27. Margulies S., Biomechanics of traumatic coma in the primate, University of Pennsylvania, PhD Dissertation, 1987.

28. Goldman, D. E. and J. B. Wells. "Longitudinal Stretch of Squid Giant Axon." Biophys. J. 41: 52a, 1983.

29. Galbraith, J. A. The Effects of Mechanical Loading on the Electrophysiology of the Squid Giant Axon. Ph.D. dissertation, University of Pennsylvania, 1988.

30. Gennarelli, T. A., L. E. Thibault, R. Tipperman, G. Tomei, R. Sergot, M. Brown, W. L. Maxwell, D. I. Graham, J. H. Adams, A. Irvine, L. M. Gennarelli, A. C. Duhaime, R. Boock and J. Greenberg. "Axonal Injury in the Optic Nerve: A Model of Diffuse Axonal Injury in the Brain." J. Neurosurg. 71: 244-253, 1989.

31. Graham, D. I., J. H. Adams, S. Legan, T. A. Gennarelli and L. E. Thibault. "The Distribution, Nature and Time Course of Diffuse Axonal Injury." Neuropathol. Appl. Neurobiol. 11: 319, 1985.

32. Thibault, L. E., T. A. Gennarelli, H. W. Tipton and D. O. Carpenter. The Physiologic Response of Isolated Nerve Tissue to Dynamic Mechanical Loads. ACEMB. 16: 176, 1974.

34. Gray, J. A. B. and J. M. Ritchie. Effects of Stretch on Single Myelinated Nerve Fibres. J. Physiol. 124: 84-99, 1954.

35. Ochs, S., R. M. Worth and S.-Y. Chan. Calcium Requirement for Axoplasmic Transport in Mammalian Nerve. Nature. 270(December): 748-750, 1977.

36. Schliwa, M., U. Euteneuer, J. C. Bulinski and J. G. Izant. Calcium Lability of Cytoplasmic Microtubules and its Modulation by Microtubule-Associated Proteins. Cell Biol. 78(2): 1037-1041, 1981.

37. Morgan, B. P., J. P. Luzio and A. K. Campbell. Intracellular Ca^{2+} and Cell Injury: A Paradoxical Role of Ca^{2+} in Complement Membrane Attack. 7: 399-411, 1986.

38. Schanne, F. A. X., A. B. Kane, E. E. Young and J. L. Farber. Calcium Dependence of Toxic Cell Death: A Final Common Pathway. Science. 206(November 9): 700-702, 1979.

39. Balentine, J. D. "Spinal Cord Trauma: In Search of the Meaning of Granular Axoplasm and Vesicular Myelin." J. Neuropathol. Exp. Neurol. 47(2): 77-92, 1988.

40. Kamakura, K., S. Ishiura, K. Suzuki, H. Sugita and Y. Toyokura. "Calcium-Activated Neutral Protease in the Peripheral Nerve, Which Requires mM Order Ca^{2+}, and Its Effect on the Neurofilament Triplet." J. Neurosci. Res. 13: 391-403, 1985.

41. Jones, H. B. and J. B. Cavanagh. "Distortions of the Nodes of Ranvier from Axonal Distension by Filamentous Masses in Hexacarbon Intoxication." J. Neurocytol. 12: 439-458, 1983.

42. Winston, FK, The Modulation of Intracellular Free Calcium Concentration by Biaxial Extensional Strains of Bovine Pulmonary Artery Endothelial Cells, Ph.D. dissertation, University of Pennsylvania, 1989

43. Barbee, KA, Cellular response of vascular smooth muscle to mechanical stimuli, Ph.D. dissertation, University of Pennsylvania, 1991

44. Thibault, LE, Gennarelli, TA, Margulies, SS, Marcus, J, Eppinger, R, The strain dependent pathophysiological consequences of inertial loading on central nervous system tissue, Proc of 1990 International IRCOBI Conf, Lyon, France

45. Chonko, A. M., J. M. Irish III and D. J. Welling. "Microperfusion of Isolated Tubules." Methods in Pharmacology. Martinez-Maldonado ed. 1978 Plenum. New York.

46. Grynkiewicz, G., M. Poenie and R. Y. Tsien. "A New Generation of Ca^{2+} Indicators with Greatly Improved Fluorescence Properties." J. Biol. Chem. 260(6)(March 25): 3440-3450, 1985.

47. Tsien, R. Y. and M. Poenie. "Fluorescence Ratio Imaging: A New Window into Intracellular Ionic Signaling." Trends Biochem. Sci. 11: 450-455, 1986.

48. Ganot, G., B. S. Wong, L. Binstock and G. Ehrenstein. "Reversal Potentials Corresponding to Mechanical Stimulation and Leakage Current in Myxicola Giant Axons." Biochim. Biophys. Acta. 649: 487-491, 1981.

49. Terakawa, S. and A. Watanabe. "Electrical Responses to Mechanical Stimulation of the Membrane of Squid Giant Axons." Pflügers Arch. 395: 59-64, 1982.

50 Hunter, C. M. Effects of Mechanical Loading on Ion Transport Through Lipid Bilayer Membranes. 1988.

51. Hashin, Z. "The Inelastic Inclusion Problem." Int. J. Engng. Sci. 7: 11-36, 1969.

52. Renkin, E. M. "Filtration, Diffusion, and Molecular Sieving Through Porous Cellulose Membranes." J. Gen. Physiol. 38: 225-243, 1955.

53. Pappenheimer, J. R., E. M. Renkin and L. M. Borrero. "Filtration, Diffusion and Molecular Sieving Through Peripheral Capillary Membranes." Am. J. Physiol. 167: 13-46, 1951.

54. Evans, E, Waugh, R and Melnik, L. "Elastic Area Compressibility Modulus of Red Cell Membrane." Biophys J. 16: 585-595, 1976.